Bioactive sol-gel glass-coated wood-derived biocarbon scaffolds

Min Yu[1,2], Elisa Fiume[3], Enrica Verné[3], Theo Saunders[1,2], Mike John Reece[1,2], Francesco Baino[3,*]

[1]School of Engineering and Material Science, Queen Mary University of London, London E1 4NS, UK

[2]Nanoforce Technology Limited, London E1 4NS, UK

[3]Institute of Materials Physics and Engineering, Applied Science and Technology Department, Politecnico di Torino, Torino, Italy

Abstract

Bioactive glass coatings were deposited for the first time onto wood-derived biocarbon scaffolds using the sol-gel technique. The cellular pore structure of the beech wood was retained during the sol-gel coating process. Owing to the presence of the bioactive glass layer, the originally bioinert biocarbon scaffold was fully covered with newly-formed hydroxyapatite (HA) upon soaking in simulated body fluid. The ability to form HA is generally accepted as the proof of *in vitro* bioactivity. This opens up the possible application of wood-derived scaffolds in biomedicine (bone repair) and biotechnology.

Keywords: biomaterials, carbon materials, sol-gel, bioactive glass, coating, scaffold.

1. Introduction

Wood exhibits excellent mechanical properties (i.e. high strength and toughness) combined with low density, owing to its high porosity (up to 90%) and cellular pore structure [1, 2]. In addition, wood has good near-net and complex shape capability, which broadens its applications from the crafts to industrial manufacturing and building construction. A variety of pore structures derived from different types of wood can also find potential application in biotechnology, including bone replacement and implant materials [3, 4], bioreactors for cell culture [5, 6], support structures for biocatalysts [7] etc. In particular, the pore channels of wood are beneficial for protein delivery and cell growth. However, despite its good biocompatibility, carbon derived from wood is known to exhibit no bioactivity due to the lack of ion-exchange phenomena to form surface hydroxyapatite (HA) upon contact with biological fluids, which is a key property for biomaterials to bond to bone [8].

* Corresponding author:
F. Baino, Tel.: +39 011 090 4668
E-mail: francesco.baino@polito.it

Bioactive silica-based glasses have been proven clinically to promote bone formation and tissue regeneration in osseous defects in orthopaedics, dentistry, maxillofacial and spinal surgery [9-12]. Bioactive glasses are generally used to coat a variety of bioinert materials in order to improve their bioactivity, including metals and ceramics [3, 13, 14].

In this work, for the first time, we demonstrated the feasibility of producing bioactive glass-coated biocarbon scaffolds derived from wood and evaluated the bioactivity of the produced materials for potential use in the context of bone repair.

2. Materials and methods

Sol-gel bioactive glass ($60SiO_2$-40CaO, mol%) was prepared using tetraethyl orthosilicate (TEOS) and $(Ca(NO_3)_2 \cdot 4H_2O$ as sources for SiO_2 and CaO, respectively. The first step was to add 2M HNO_3 solution (1.2 mL) into deionized water (7.2 mL) and mix for 5 min at a stirring speed of 200 rpm; the second step was to add TEOS (11.67 mL) and mix for 1.5 h at 200 rpm; the final step was to add $Ca(NO_3)_2 \cdot 4H_2O$ (8.22 g) and mix for 1 h at 200 rpm. All of the chemicals were purchased from Sigma-Aldrich and used as received. The biocarbon scaffolds were prepared by the pyrolysis of beech wood, as reported elsewhere [15]. The glass coating was then prepared by dipping the biocarbon scaffolds for ~12 h into the prepared sol and then performing a heat treatment in a tubular furnace (700°C for 3 h, heating rate of 5°C/min) under inert atmosphere (Ar) to form the bioactive glass, preserving the carbonaceous skeleton.

The *in vitro* bioactivity testing was carried out by soaking triplicate samples in a simulated body fluid (SBF) for 24 h, 48 h, 7 days and 14 days at 37°C. The SBF was prepared according to the Kokubo's procedure [16]. At each time point, the samples were taken out from the SBF and gently rinsed in deionized water. Every 48 h, the SBF was replaced with fresh solution in order to simulate fluid circulation in human body. Before refreshing, the pH was monitored to evaluate the ion exchange between the solution and the material surface.

A scanning electron microscope (SEM, Supra 40, ZEISS) was used to reveal the microstructure of the samples before and after immersion in the SBF, and energy dispersive spectroscopy (EDS) in order to determine the composition of the surface. Detection of calcium phosphate phases formed upon *in vitro* tests was performed by X-ray diffraction (XRD) analysis (X'Pert Pro PW3040/60 diffractometer, PANalytical) using the X'Pert HighScore software (2.2b) equipped with the PCPDFWIN database (http://pcpdfwin.updatestar.com).

3. Results and discussion

Fig. 1 reports SEM images of the glass-coated biocarbon scaffold. As shown in Fig. 1a and b, the scaffold exhibited two types of spheroidal macropores ranging within 50-100 μm (unidirectional pores along the wood growth direction) and 5-10 μm (throughout the solid walls), respectively, which are in good agreement with our previous work [15]. The original pore structure derived from wood was retained in the sample body after sol-gel coating. Only a small proportion of the macropores were observed to be fully filled (occluded) by the glass, as shown in the red square in Fig. 1b. The presence of the glass coating on the carbon walls can be seen in Fig. 1b and c. It is worth noting that the glass coating was not strongly attached to the pore walls in the scaffold, as shown in Fig. 2c. This might have resulted from the shrinkage of the gel during the heat treatment. The bioactive glass exhibited submicrometric structure of assembled spherical nanoparticles (~50 nm), which is typical of sol-gel-derived materials (Fig.2d) and in good agreement with the results from the literature [17]. The compressive strength of this wood-derived biocarbon scaffold was ~27MPa, which was reported in our previous work [15].

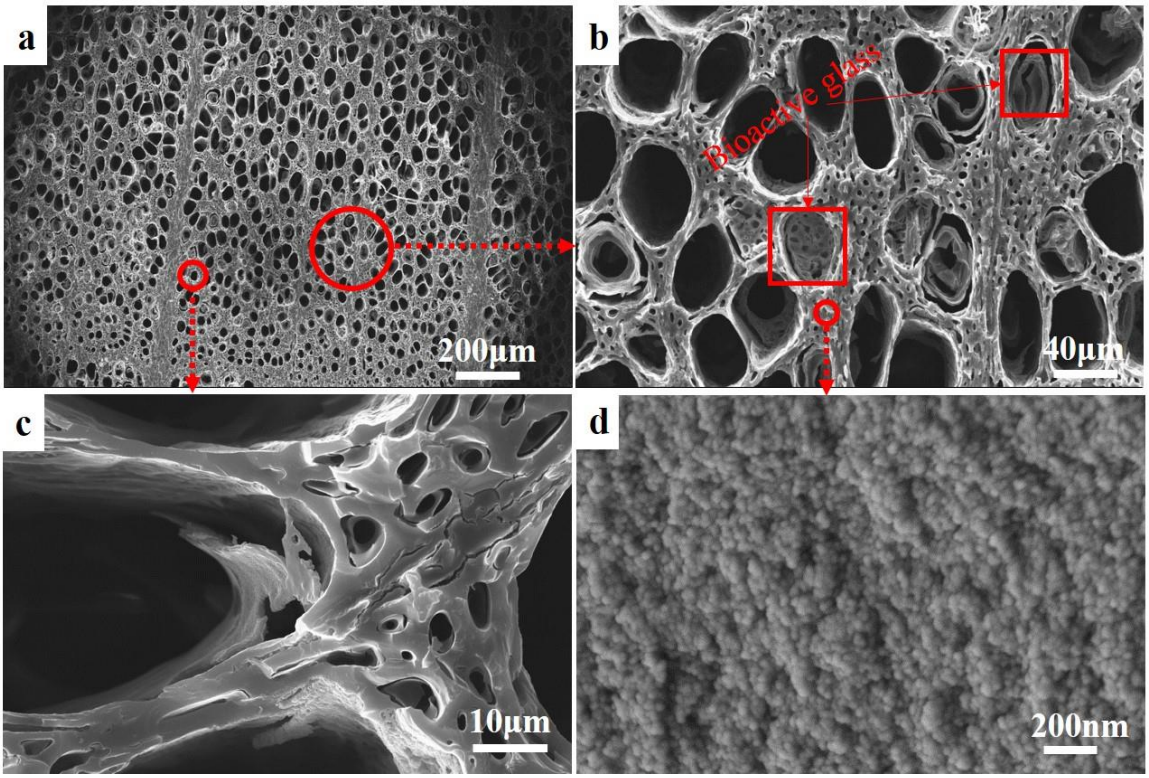

Fig. 1. SEM micrographs of the bioactive glass-coated biocarbon scaffold (surface) at different magnifications.

Fig. 2 shows the pH values of the SBF after soaking the samples over the testing period. The pH value of the SBF increased to 7.65 after soaking the sample for 2 days, in accordance with the ion-exchange phenomena

leading to the formation of HA on the sample surface. Then, the pH of the SBF tended to stabilize and remained constant at ~7.54 with the increase of immersion time from 6 to 14 days. No problems of toxicity to cells/tissues due to these moderate pH increments towards alkalinity in an in-vivo scenario would be expected.

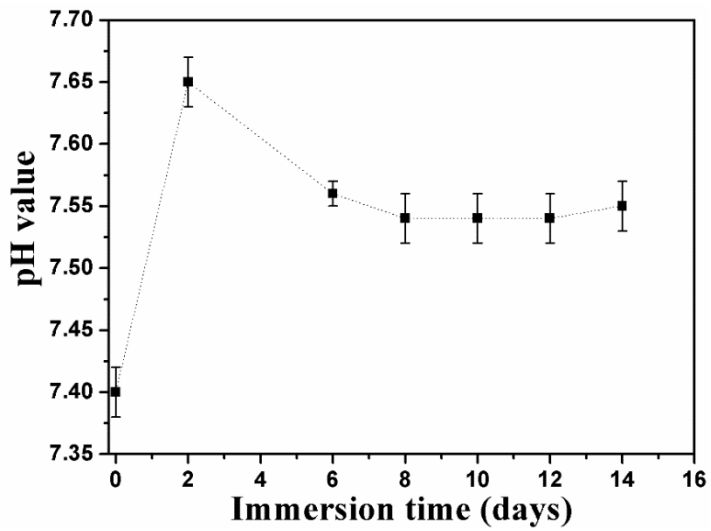

Fig. 2 The pH value of the SBF solution as a function of soaking time.

Fig. 3 shows SEM images of bioactive glass-coated biocarbon scaffold after soaking in SBF for 24 and 48 h. The EDS analysis reveals the formation of a calcium phosphate layer on the surface of the scaffolds with a Ca/P atomic ratio of ~1.65, which is similar to that of stoichiometric HA (~1.67). The struts/walls of the biocarbon scaffolds were fully coated with globular HA showing a "cauliflower morphology" and retained the original pore structures derived from wood, as shown in Fig. 3a and b. The HA exhibited a nanocrystalline nature with needle-like crystals (Fig. 3c), which is the typical morphology of the HA formed on sol-gel glasses [18]. The biocarbon struts were fully covered with the HA layer, indicating excellent bioactivity for the glass-coated biocarbon scaffold.

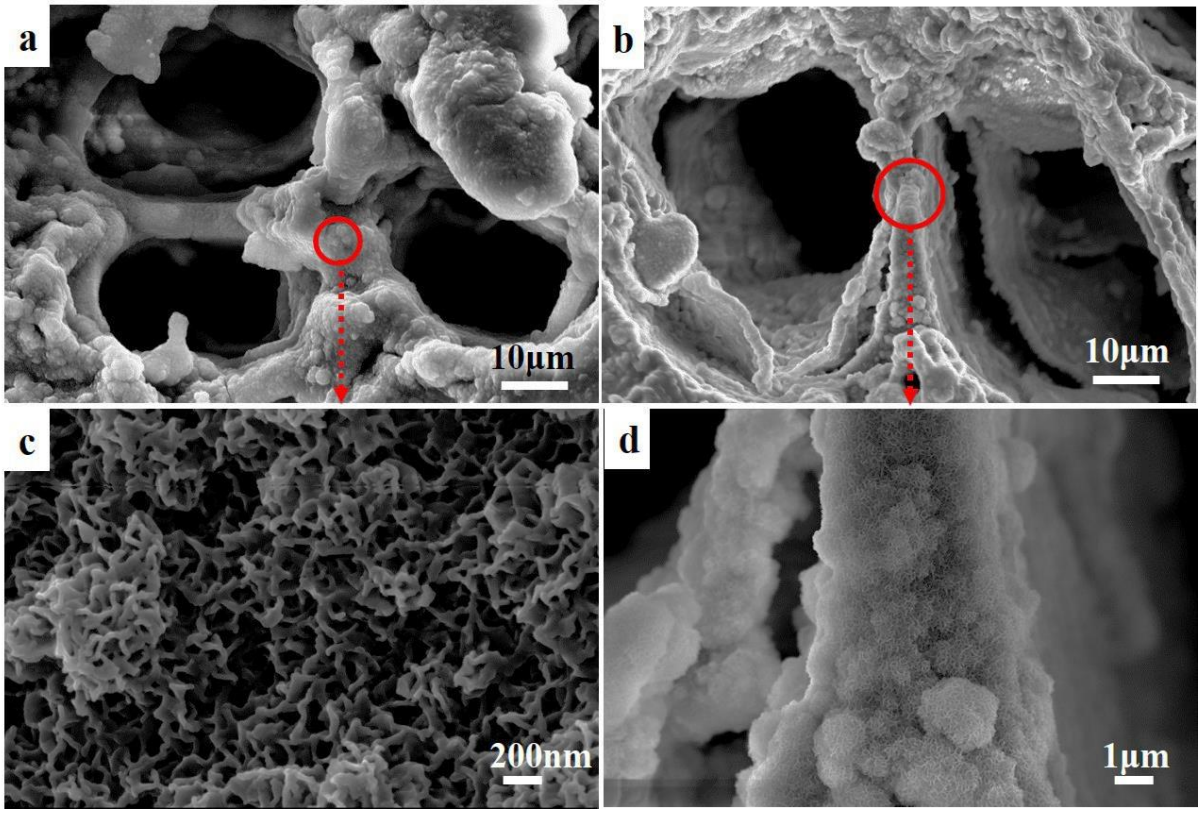

Fig.3. SEM micrographs of the bioactive glass-coated biocarbon scaffold (surface) after immersing in SBF for 24 h (a and c) and 48 h (b and d). (c) and (d) are the high-magnification images of (a) and (b), respectively.

Fig. 4 shows XRD patterns of the scaffolds after immersing in SBF for different times. All of the samples exhibited the characteristic peaks (at 26.4°, reflection (002), and 32.3°, reflection (211)) of crystalline HA formed in SBF, which further confirmed the results from the SEM-EDS analysis (Fig. 3). This mainly resulted from the ion exchange between samples and solution, according to the bioactivity mechanism proposed for bioactive glasses [19]. The HA peaks detected are generally quite broad due to the nanocrystalline nature of the newly-formed phase (which mimics bone bioapatite [20]), but they became sharper with the increase of immersion time from 24 h to 2 weeks, which is in good agreement with previous results from the literature [21]. This might result from the continuous reaction between scaffold and solution, as confirmed by the increased pH value of SBF (Fig. 2).

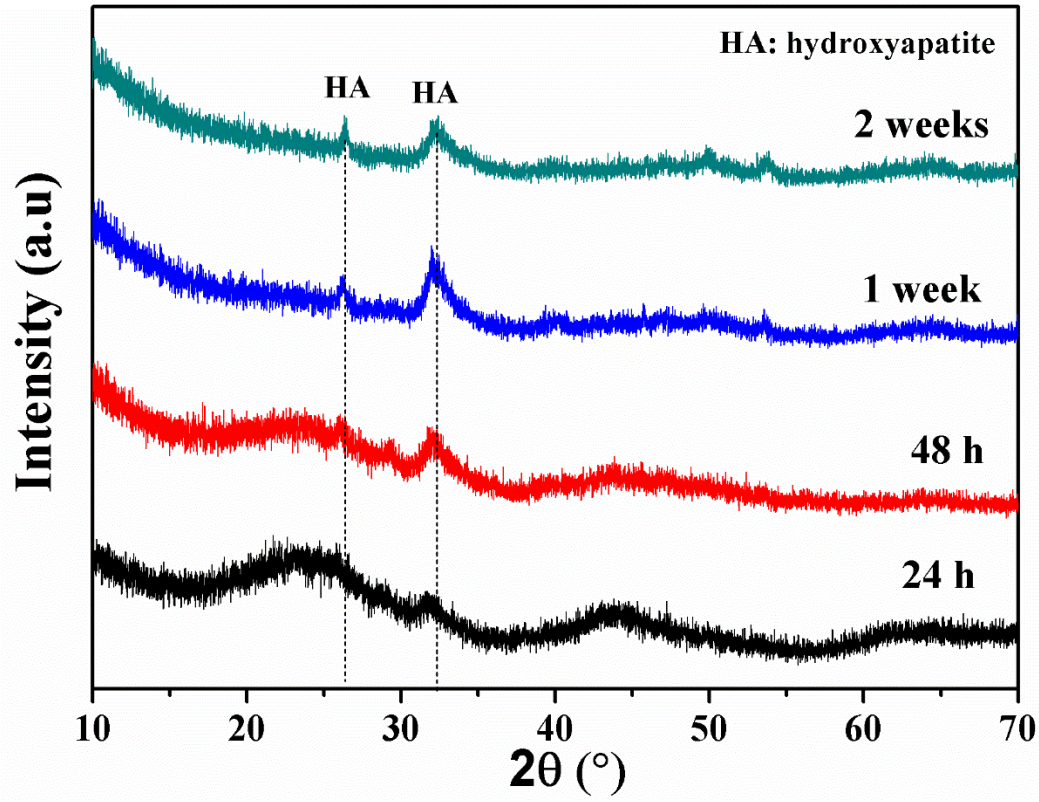

Fig.4. XRD patterns of the bioactive glass-coated scaffold after immersing in SBF solution for different time (24 h, 48 h, 1 week and 2 weeks).

4. Conclusions

A sol-gel bioactive glass coating was successfully deposited, for the first time, onto bioinert wood-derived biocarbon scaffolds. The hierarchical pore structure (pore size: ~50 μm and ~5 μm) derived from beech wood was retained in the glass-coated scaffolds. The glass layer was able to impart bioactive properties to the under-laying carbon skeleton, as confirmed by the formation of nanocrystalline HA on the pore walls of the samples after immersion in SBF for above 24 h. These results suggest a potential for application in bone tissue repair.

Acknowledgements

M.Y. acknowledges the support of the EU's H2020 Programme through a Marie Skłodowska-Curie Innovative Training Network ("CoACH-ETN", http://www.coach-etn.eu, G.A. no. 642557).

References

[1] M. Zhu, J. Song, T. Li, A. Gong, Y. Wang, J. Dai, Y. Yao, W. Luo, D. Henderson, L. Hu, Advanced Materials ~~(2016)~~*28* (2016) 5181-5187.

[2] V. Yukhymchuk, V. Kiselov, M.Y. Valakh, M. Tryus, M. Skoryk, A. Rozhin, S. Kulinich, A. Belyaev, Journal of Physics and Chemistry of Solids 91 (2016) 145-151.

[3] P. Gonzalez, J. Serra, S. Liste, S. Chiussi, B. Leon, M. Perez-Amor, J. Martınez-Fernández, A. de Arellano-Lopez, F. Varela-Feria, Biomaterials 24(26) (2003) 4827-4832.

[4] J. Qian, Y. Kang, Z. Wei, W. Zhang, Materials Science and Engineering: C 29(4) (2009) 1361-1364.

[5] I. Martin, D. Wendt, M. Heberer, TRENDS in Biotechnology 22(2) (2004) 80-86.

[6] L. Ma, C. Gao, Z. Mao, J. Zhou, J. Shen, X. Hu, C. Han, Biomaterials 24(26) (2003) 4833-4841.

[7] C.R. Rambo, H. Sieber, Advanced Materials 17(8) (2005) 1088-1091.

[8] T. Fu, L.-P. He, Y. Han, K.-W. Xu, Y.-W. Mai, Materials Letters 57(22) (2003) 3500-3503.

[9] M. Yu, K. Zhou, F. Zhang, D. Zhang, Ceramics International 40(8) (2014) 12617-12621.

[10] F. Baino, E. Fiume, M. Miola, E. Verné, International Journal of Applied Ceramic Technology.

[11] Q.Z. Chen, I.D. Thompson, A.R. Boccaccini, Biomaterials 27(11) (2006) 2414-2425.

[12] A. Hoppe, N.S. Güldal, A.R. Boccaccini, Biomaterials 32(11) (2011) 2757-2774.

[13] J. Gomez-Vega, E. Saiz, A. Tomsia, G. Marshall, S. Marshall, Biomaterials 21(2) (2000) 105-111.

[14] T. Kokubo, Biomaterials 12(2) (1991) 155-163.

[15] M. Yu, E. Bernardo, P. Colombo, A.R. Romero, P. Tatarko, V.K. Kannuchamy, M.-M. Titirici, E.G. Castle, O.T. Picot, M.J. Reece, Ceramics International 44(11) (2018): 12957-12964 ~~(2018)~~.

[16] T. Kokubo, H. Takadama, Biomaterials 27(15) (2006) 2907-2915.

[17] J.R. Jones, Acta biomaterialia 23 (2015) S53-S82.

[18] M. Vallet-Regí, e. Romero, C. Ragel, R. LeGeros, Journal of Biomedical Materials Research 44(4) (1999) 416-421.

[19] L.L. Hench, Annals of the New York academy of sciences 523(1) (1988) 54-71.

[20] A.L. Boskey, Elements 3(6) (2007) 385-391.

[21] A. Balamurugan, G. Sockalingum, J. Michel, J. Fauré, V. Banchet, L. Wortham, S. Bouthors, D. Laurent-Maquin, G. Balossier, Materials Letters 60(29) (2006) 3752-3757.